Charles R. Pierce
Regulatory Affairs Director

Southern Nuclear
Operating Company, Inc.
40 Inverness Center Parkway
Post Office Box 1295
Birmingham, AL 35242

Tel 205.992.7872
Fax 205.992.7601

SOUTHERN NUCLEAR
A SOUTHERN COMPANY

MAY 23 2016

Docket Nos.: 50-321

NL-16-0767

U. S. Nuclear Regulatory Commission
ATTN: Document Control Desk
Washington, D. C. 20555-0001

Edwin I. Hatch Nuclear Plant – Unit 1
Crack Growth Analysis of the Recirculation Inlet Nozzles
1B31-1RC1-12BR-E-5 Weld Overlay

Ladies and Gentlemen:

Edwin I. Hatch Nuclear Plant (HNP) Alternative HNP-ISI-ALT-15-01 was approved by the Nuclear Regulatory Commission (NRC) on December 18, 2015 to allow installation of full structural weld overlays on four welds during the Unit 1 spring 2016 refueling outage. This Alternative stipulated that, should a flaw be found in the upper 25% of the original weld or base material, Southern Nuclear Operating Company (SNC) would provide an evaluation of flaw growth to the NRC within 90 days of startup. During the refueling outage, an axial indication was identified by Liquid Penetrant test on the partially grounded surface of the previously installed weld overlay, which suggested an indication with a through-wall depth greater than the originally assumed 75% through-wall flaw in recirculation inlet nozzle 1B31-1RC1-12BR-E-5 dissimilar metal weld. The Enclosure transmits the required evaluation per the Alternative.

This letter contains no NRC commitments. If you have any questions, please contact Ken McElroy at (205) 992-7369.

Respectfully submitted,

C R Pierce

C. R. Pierce
Regulatory Affairs Director

CRP/RMJ

Enclosure: Revision 1 of Crack Growth Analysis on the Recirculation Inlet Nozzles

cc: Southern Nuclear Operating Company
Mr. S. E. Kuczynski, Chairman, President & CEO
Mr. D. G. Bost, Executive Vice President & Chief Nuclear Officer
Mr. D. R. Vineyard, Vice President – Hatch
Mr. M. D. Meier, Vice President – Regulatory Affairs
Mr. D. R. Madison, Vice President – Fleet Operations
Mr. B. J. Adams, Vice President – Engineering
Mr. G. L. Johnson, Regulatory Affairs Manager - Hatch
RTYPE: CHA02.004

U. S. Nuclear Regulatory Commission
Ms. C. Haney, Regional Administrator
Mr. M. D. Orenak, NRR Project Manager – Hatch
Mr. D. H. Hardage, Senior Resident Inspector – Hatch

Edwin I. Hatch Nuclear Plant – Unit 1
Crack Growth Analysis of the Recirculation Inlet Nozzles
1B31-1RC1-12BR-E-5 Weld Overlay

Enclosure

Revision 1 of Crack Growth Analysis on the Recirculation Inlet Nozzles

Structural Integrity Associates, Inc.®	File No.: 1500503.316
CALCULATION PACKAGE	**Project No.: 1500503** Quality Program Type: ☒ Nuclear ☐ Commercial

PROJECT NAME:
Hatch 1 Recirculation Inlet Nozzle Weld Overlay

CONTRACT NO.:
SNG10110967, Rev.1

CLIENT:	**PLANT:**
Southern Nuclear Company (SNC)	Edwin I. Hatch, Unit 1

CALCULATION TITLE:
Crack Growth Analyses of the Recirculation Inlet Nozzles N2C and N2E Weld Overlay

Document Revision	Affected Pages	Revision Description	Project Manager Approval Signature & Date	Preparer(s) & Checker(s) Signatures & Date
0	1 - 27 A-1 - A-3	Initial Issue	Richard Bax 11/17/15	Preparers: Richard Bax 11/17/15 Minji Fong 11/17/15 Checker: Kevin Wong 11/17/15
1	1, 3-5, 7, 9, 13-16, 19, 21, A-3	Additional crack growth evaluation to account for an indication at weld 1B31-1RC1-12BR-E-5	Terry Herrmann 03/22/16	Minji Fong 03/22/16 Richard Bax 03/22/16

Table of Contents

List of Tables

List of Figures

1.0 OBJECTIVE

The objective of this calculation package is to evaluate crack growth in the recirculation inlet nozzle to support the application of a preemptive full structural weld overlay (FSWOL) on the nozzle-to-safe end dissimilar metal welds (DMW) 1B31-1RC1-12BR-C-5 and 1B31-1RC1-12BR-E-5 at the Edwin I. Hatch Nuclear Plant, Unit 1 (HNP1). Loads considered are internal pressure, external piping loads, thermal transients, and weld residual stresses. Both fatigue crack growth (FCG) and Intergranular Stress Corrosion Cracking (IGSCC) are considered. FCG is due to cyclic loading, while IGSCC is due to sustained loading at steady state normal operating conditions (NOC).

Revision 1: This calculation was revised to add an additional crack growth evaluation due to the presence of an ultrasonic examination based axial indication that is greater than the originally assumed 75% through-wall flaw in the recirculation inlet nozzle 1B31-1RC1-12BR-E-5 DMW.

2.0 TECHNICAL APPROACH

Stress intensity factors (K distributions) for a semi-elliptical axial flaw and a postulated 360° circumferential flaw, both located connected to the inside surface, are determined using representative fracture mechanics models (see Section 4.1). The K distributions due to the various applied loads are computed as a function of postulated crack depth and linearly superimposed for the various operating states. Stresses from the applied loads that contribute to FCG and IGSCC are compiled from supporting calculations (References 1 and 2).

For postulated circumferential and axial flaws, an initial flaw depth of 75% of the original base metal thickness is assumed for computing crack growth in the nozzle with a FSWOL [3].

Appendix 9 of Reference 4, "Applicable Ultrasonic Examination History," indicates that weld 1B31-1RC1-12BR-C-5 first had an indication in 1988 of an axial flaw that was 0.15 inches through-wall. Subsequent examinations, since the application of the original weld overlay, in 1988, 1990, 1991 and 1994 showed that the indication had not grown. The wall thickness in the area of the flaws is 1.2 inches [4, Appendix 9], which means the maximum indication depth of 0.15 inch at weld 1B31-1RC1-12BR-C-5 is 12.5% through-wall. As stated earlier, an initial axial flaw of 75% of the original base metal thickness is considered for nozzle with a FSWOL. Therefore, the presence of the pre-existing flaws at weld 1B31-1RC1-12BR-C-5 are bounded and need not be specifically evaluated.

Similarly, weld 1B31-1RC1-12BR-E-5 first had an indication in 1988 of an axial indication that was 0.85 inches through-wall. Subsequent to the application of the original weld overlay, a 2006 ultrasonic examination sized the indication at 0.60 inches through-wall. However, during the post-FSWOL ultrasonic examination, a 100% through-wall axial indication was recorded [15, pg. 2 of 43]. It will, therefore, be necessary to evaluate an initial flaw depth of 100% of the original base metal thickness for an axial flaw to account for this indication.

Since the assumed initial flaw depth (75% of the original base metal thickness) starts in the DMW material, crack growth rates for Alloy 182, applicable to a BWR environment, are used to calculate the propagation in the thickness direction of the postulated cracks. The stress intensity factors are determined at 75% of the original base metal thickness first. Then, if the stress intensity factors are greater than zero, the time it takes for an initial flaw of 75% of the original base metal thickness to grow to original base metal to FSWOL interface is computed and reported herein.

The stress intensity factors at 100% of the original base metal thickness, for an axial flaw, are also determined. If the stress intensity factors at 100% of the original base metal are greater than zero, the time it takes for an initial axial flaw of 100% of the original base metal thickness to grow to 75% of the total thickness, including the FSWOL, is computed and reported herein.

3.0 DESIGN INPUTS

Input data for the crack growth evaluation are the stress distributions due to applied loads that were determined in References 1 and 2 for the recirculation inlet nozzle. These stress distributions are used to determine K distributions (see Section 4.1). Stresses are extracted within the DMW, as shown in Figure 2, and mapped onto the section thickness shown in Figure 1. Three paths were selected to represent the DMW region: a path near the nozzle interface within the weld butter, a path in the approximate center of the susceptible material, and a path near the safe end side of the weld. The applied loads are internal pressure, piping interface loads, local thermal gradient stresses due to thermal transients, and weld residual stresses. These loads are described in the following subsections.

3.1 Stresses due to Internal Pressure

In the thermal and mechanical stress analysis calculation package [1], a unit internal pressure load (1,000 psi) was applied to the recirculation inlet nozzle finite element model with the minimum overlay dimensions. The resulting through-wall stress distributions due to unit pressure were extracted from paths within the DMW (see Figure 2). The K distributions resulting from these stresses are conservatively scaled by the actual maximum and minimum pressure values that occur during the specific transient (see Table 2). The K distributions in the DMW were determined using the methodology in Section 4.1.1.

3.1.1 Crack Face Pressure

A constant through-wall stress of 1 ksi is applied to account for the internal pressure acting on the crack face. The constant through-wall stress is conservatively scaled by the actual minimum and maximum pressure values that occur of each transient (see Table 2) for FCG evaluation (see Section 4.2) and by the normal operating pressure value for the IGSCC evaluation (see Section 4.3).

3.2 Stresses due to Piping Interface Loads

The bounding piping interface loads were determined in the design loads calculation package [5, Table 3] and reproduced in Table 1 of this calculation. Finite element analyses for an applied unit axial force (1,000 lbs) and unit moments (1,000 in-lb) at the free end of the modeled piping for the recirculation inlet nozzle finite element model with the minimum overlay dimensions were performed in the Reference 1 analyses. Because unit forces and unit moments were analyzed in Reference 1, the resulting K distributions due to the unit force are scaled to actual values of axial force (FA in Table 1) and K distributions for the unit moments are scaled to the square root sum of the squares (SRSS) of the bending moment values (MB and MC in Table 1). The unit force and unit moment K distributions are also conservatively scaled by to the appropriate maximum and minimum temperatures for each transient (see Table 2) using the temperature scaling factor described in Section 4.2 of Reference 5. The K distributions in the DMW were determined using the methodology in Section 4.1.1.

3.3 Stresses due to Thermal Transients

Bounding thermal transients for crack growth analysis are shown in Table 2, which were developed in the design loads calculation package [5] and were analyzed in the thermal and mechanical stress analysis calculation package using the recirculation inlet nozzle finite element model with the maximum overlay dimensions [1]. K distributions were determined using the stress distributions due to thermal transients in the DMW. It should be noted that since the finite element models developed in Reference 6 have different material properties modeled, bimetallic stresses are already captured and need not be evaluated separately. It should also be noted that during a transient, it is possible to have more than one maximum-minimum stress pair (i.e. more than one peak-valley pair). The number of cycles for this kind of transient is multiplied by the number of peak-valley pairs for that particular transient. Table 2 shows the number of peak-valley pairs for each transient. The K distributions in the DMW were determined using the methodology in Section 4.1.2.

3.4 Weld Residual Stresses

Through-wall axial and hoop weld residual stresses were obtained from the residual stress analysis [2] for the recirculation inlet nozzle finite element model with the minimum overlay dimensions. These stress distributions are shown in Figure 3. The 70°F residual stress and the steady state normal operating stresses (residual stresses + normal operation pressure stresses + normal operation temperature stresses) were also obtained from the residual stress analysis [2] and are used to determine the K distributions at 70°F for FCG and at steady state NOC for the IGSCC evaluation (see Section 4.3). The K distributions in the DMW for weld residual stress at 70°F and at NOC were determined using the methodology in Section 4.1.1.

4.0 CALCULATIONS

The major components of the crack growth evaluation are discussed in the following subsections.

4.1 Stress Intensity Factors

4.1.1 Unit Loads and Weld Residual Stresses

The through-wall axial and hoop stress distributions for the unit pressure, unit force, unit moments, weld residual at 70°F and weld residual at NOC were input into **pc-CRACK** [7], a fracture mechanics program developed by Structural Integrity Associates under its quality assurance program.

The axial stress distributions from the Reference 1 and 2 analyses were input into **pc-CRACK**, and using "Crack Model: 301 - Full-Circumferential Crack in Cylinder on the Inside Surface," as shown in Figure 4, the K distributions were determined.

The hoop stress distributions from the Reference 1 and 2 analyses were input into **pc-CRACK**, and using "Crack Model: 305 - Semi-Elliptical Longitudinal Crack in Cylinder on the Inside Surface (API 579)," as shown in Figure 5, the K distributions were determined for a number of a/c ratios.

The three paths shown in Figure 2 have varying lengths, but the minimum thickness shown in Figure 1 of 1.743 inches (1.203 inches of the base metal thickness plus 0.54 inches of the minimum weld overlay thickness) is used. **pc-CRACK** normalizes the applied stresses to produce the K distribution for the given thickness and stress cases.

The as-built FSWOL thicknesses were measured and documented in Reference 16. The average measured overlay thicknesses are 0.5229 inch at Station B [16, 17] and 0.6174 inch at Station C [16, 17] for weld 1B31-1RC1-12BR-C-5 [16, Component ID: 1B31-1RC1-12BR-C-5, Sheet 3]. For weld 1B31-1RC1-12BR-E-5 [16, Component ID: 1B31-1RC-12BR-E-5, Sheet 3], the average measured overlay thicknesses are 0.5254 inch at Station B [16, 17] and 0.7119 inch at Station C [16, 17]. For both nozzles, the as-measured thicknesses are greater than the minimum values of 0.44 inch at Station B and 0.54 inch at Station C [17].

In the case of weld 1B31-1RC1-12BR-E-5, the base wall thickness of the DMW is 1.203 inches [6, Figure 2]. The ultrasonically-measured, remaining ligament above the 100% through-wall flaw is 17.4 mm (0.6850 inch) [15, pg. 2 of 43]. Thus, the final a/t ratio at the axial flaw is (1.203)/(1.203+0.6850) = 0.64, which is less than ASME Code, Section XI, Appendix C limit of 0.75 [9].

This is conservative as the 1.743 inch analysis thickness is less than or equal to the actual path lengths. The through-wall stress files for the three paths, generated in References 1 and 2 are listed in Appendix A.

Note that because the stresses were input in terms of psi, the resulting K values are in terms of psi$\sqrt{in}$ and will need to be converted to ksi$\sqrt{in}$.

See Appendix A for the **pc-CRACK** input and output files.

4.1.2 Stress Intensity Factors – Thermal Transient Stresses

The thermal transient evaluations performed in Reference 1 results in many individual time points within each transient, each of which has through-wall hoop and axial stress data extracted for the three paths shown in Figure 2. In order to process all of the thermal transient data and to determine the K_{max} and K_{min} for each transient for multiple crack depths and flaw aspect ratios, the results are input into **SI-TIFFANY** [8], a specialized fracture mechanics program developed by Structural Integrity Associates under its quality assurance program.

SI-TIFFANY reads in the time history of through-wall hoop and axial stresses for each transient. The program then determine K for every time point and for every flaw depth, and defined aspect ratios (aspect ratio is only valid for the axial flaw as the circumferential flaw is assumed to be 360°). The program then selects the highest K and lowest K for each flaw depth and each flaw aspect ratio for all time points and produces two files.

The "*.mnn" file tabulates the wall thickness versus smallest K_{min} for the given path length evaluated. In the case of the axial flaw, the "*.mnn" file provides the wall thickness versus smallest K_{min} for each designated aspect ratio.

The "*.mxn" file is the same as the "*.mnn," except that the K_{max} values are tabulated.

The three paths shown in Figure 2 have varying lengths, but the minimum thickness shown in Figure 1 of 1.743 inches is used. **SI-TIFFANY** normalizes the applied stresses to produce the K distribution for the given thickness and stress cases. This is conservative as the 1.743 inch analysis length is less than or equal the actual path lengths. The through-wall stress files for the three paths, generated in Reference 1, are listed in Appendix A.

Note that the input file for **SI-TIFFANY** provides the option to scale the input stress such that K-values can be output as desired, e.g., psi$\sqrt{in}$ or ksi$\sqrt{in}$. For this calculation all of the results generated by **SI-TIFFANY** are in terms of ksi$\sqrt{in}$.

See Appendix A for the **SI-TIFFANY** input and output files.

4.2 Fatigue Crack Growth

The FCG laws used in this analysis are discussed in the following subsections. The sequence of events for FCG is shown in Table 2 and is computed based on a yearly basis. Thus the cycles shown in Table 2 are divided by 40 years [5] for a yearly block (period) FCG calculation. In FCG there is no requirement for load pairing between transients (that occur at different times throughout the plant operating term) per the ASME Code, Section XI [9]. Each thermal transient that was analyzed in the thermal and mechanical stress analysis calculation package [1] is analyzed sequentially per Table 2. This approach is consistent with Subsubarticle C-3210 of the ASME Code, Section XI [9].

In FCG, the individual terms that constitute nominal K_{max} and K_{min} for the calculation of ΔK (see Section 4.2.1 and Section 4.2.2) are summarized in the following tabulations.

K_{max}	K_{min}
$K_{residual@70}$	$K_{residual@70}$
$K_{dead\ weight}$	$K_{dead\ weight}$
$K_{pressure\ max}$	$K_{pressure\ min}$
$K_{crack\ face\ pressure\ max}$	$K_{crack\ face\ pressure\ min}$
$K_{thermal\ piping\ load\text{-}max}$	$K_{thermal\ piping\ load\text{-}min}$
$K_{thermal\ transient\ max}$	$K_{thermal\ transient\ min}$
$K_{OBE\ max}$	$K_{OBE\ min}$

The individual Ks for nominal K_{max} are combined (summed) with all appropriate scale factors (see Sections 3.1 and 3.2) applied. Similarly, the individual Ks for nominal K_{min} are combined (summed) with all appropriate scale factors applied. ΔK is computed by taking the difference of the resulting summed K_{max} and K_{min}. Note that $K_{residual@70}$ and $K_{dead\ weight}$ are constant loads and therefore, do not contribute to the ΔK range. However, $K_{residual@70}$ and $K_{dead\ weight}$ affect the value of the R-ratio (see Sections 4.2.1 and Section 4.2.2).

Because there is a known flaw already present in the heat affected zone of the stainless steel safe end, directly adjacent to the DMW, the crack growth will also be determined using the stainless FCG and IGSCC laws, but only for the Path 3 and Path 8 data, which will be conservatively treated as representative for the stainless steel heat affected zone region.

Note that all crack growth evaluations are based on the minimum wall thickness shown in Figure 1, which is conservative and represents the minimum allowed overlay dimensions. For the 100% through-wall axial flaw case, the stainless steel case is not relevant and is, therefore, not evaluated.

4.2.1 Alloy 82/182 Fatigue Crack Growth Law

Fatigue crack growth is calculated using the rate for Alloy 182 welds exposed to a BWR environment per NUREG/CR-6721 [10]. This crack growth rate is shown in Equation (1). Reference 10 indicates that the fatigue crack growth rate for Alloy 600 in air may be used with a factor of 2 applied for Alloy 182 weld metal in air. An additional term (the second term in Equation (1)) is to account for a BWR water environment per Reference 10.

$$\left(\frac{da}{dN}\right)_{env\ A182} = \left(\frac{da}{dN}\right)_{air\ A182} + A \cdot T_r^{1-m}\left(\frac{da}{dN}\right)^m_{air\ A182} \qquad (1)$$

where:

$(da/dN)_{air\ A182}$	$= 2*C_{A600}\ (1\text{-}0.82R)^{-2.2}\ (\Delta K)^{4.1}$, **m/cycle** (multiply by 39.36996 for **in/cycle**)
A	$= 4.4 \times 10^{-7}$ (per Reference 10, Figure 9(a))
T_r	= rise time, seconds
m	= 0.33 (per Reference 10, Figure 9(a))
C_{A600}	$= 4.835 \times 10^{-14} + 1.622 \times 10^{-16} T - 1.49 \times 10^{-18} T^2 + 4.355 \times 10^{-21} T^3$
T	= temperature inside pipe, °C
R	= R-ratio = (K_{min}/K_{max})
ΔK	= $K_{max} - K_{min}$ = range of stress intensity factor, MPa$\sqrt{m}$

Conservatively using the maximum temperature, 553°F, from all transients in Table 2, the C_{A600} coefficient is calculated as:

$$C_{A600} = 4.19 \times 10^{-13}$$

A rise time of 16,056 seconds, corresponding to the maximum stress response time of the Start up + First Part of Turbine Roll & Increase to Power transient, is used for all FCG evaluations. The use of a shorter rise time would produce less crack growth, which makes the chosen value conservative for the other transients analyzed herein.

The crack growth law listed above cannot be directly entered into **pc-CRACK**. Therefore, the da/dN values, for various R-ratios, are calculated in an Excel spreadsheet, *1500503.316.xlsm,* and entered into **pc-CRACK** as a table of da/dN values versus R-ratio.

Due to the beneficial compressive effects of the FSWOL, the total K_{max} and total K_{min} values for some transients can both be negative. In such cases, the **pc-CRACK** generated R-ratio can be greater than 1.0, which will generate an error. In such cases, a constant R-ratio of 0.9 is conservatively used for the FCG evaluation.

FCG is computed using the sequence of events shown in Table 2 and is calculated on a yearly basis. Thus the cycles shown in Table 2 are divided by 40 years [5] for a yearly block FCG calculation.

4.2.2 Stainless Steel Fatigue Crack Growth

Crack growth in the stainless steel is calculated using the austenitic steel fatigue crack growth law in air from Article C-3210 of the ASME, Section XI [9]. A JPVT paper [11] indicates a factor of 10 may be applied to the crack growth law in air to account for a BWR environment.

$$\frac{da}{dt} = 10 \cdot C_0 \cdot (\Delta K)^n \text{, units of in/cycle} \qquad (2)$$

where,

C_0 = C·S
C = 10^[-10.009 + 8.12x10^{-4}T – 1.13x10^{-6}T^2 + 1.02x10^{-9}T^3]
S = 1.0 when R ≤ 0
= 1.0 + 1.8R when 0 < R ≤ 0.79
= -43.35 + 59.79R when 0.79 < R ≤ 1.0
T = metal temperature in °F
R = R-ratio = (K_{min}/K_{max})
ΔK = $K_{max} – K_{min}$ = range of stress intensity factor, ksi√in
n = 3.3 per Section XI, Appendix C [9]

Conservatively using the maximum temperature of the fluid, 553°F, from all transient in Table 2, the temperature dependent C coefficient is calculated as:

C = 1.85 x 10^{-9}

4.3 IGSCC Growth

IGSCC is a time dependent phenomenon and occurs during sustained loading conditions. Given that the great majority of plant operation is at steady state NOC, IGSCC is defined by the stress condition at NOC (see Figure 6). IGSCC is defined to be active when the K_I at steady state NOC is a positive number. If IGSCC is active, crack growth is determined for a one-year time period, similar to the FCG calculation, using the crack growth rate in Section 4.3.1 and Section 4.3.2. Alternating one-year blocks (periods) of FCG and IGSCC growth (if IGSCC is active) are used to calculate total cumulative crack growth.

For IGSCC, the K_I is calculated in the following tabulation.

K_I
$K_{residual@NOC}$
$K_{crack\ face\ pressure@NOC}$
$K_{deadweight}$
$K_{thermal\ expansion\_piping\ load@NOC}$

The K distributions at steady state normal operating conditions (NOC) are shown in Figure 6 and are used to determine if IGSCC is active ($K_I > 0$).

Because there is a known flaw already present in the heat affected zone of the stainless steel safe end, directly adjacent to the DMW. The IGSCC will also be determined using the stainless IGSCC growth law, but only for the Path 3 and Path 8 data, which will be conservatively treated as representative for the stainless steel heat affected zone region.

4.3.1 *Alloy 182 IGSCC Growth Law*

BWRVIP-59-A [12] provides stress corrosion crack growth laws for high nickel base austenitic alloys for different BWR water chemistry conditions. Because of the limitation of the IGSCC equation format in **pc-CRACK**, Equation (3) is applied first and Equation (4) is subsequently applied if the stress intensity factor is larger than 25 ksi√in.

$$\frac{da}{dt} = C_0 K_I^n \text{ in/hr for } K_I \le 25 \text{ ksi}\sqrt{\text{in}} \quad (3)$$

$$\frac{da}{dt} = C_1 \text{ in/hr for } K_I > 25 \text{ ksi}\sqrt{\text{in}} \quad (4)$$

where,

K_I = stress intensity factor at flaw tip, ksi√in
C_0 = 3.2×10^{-10} for HWC, 1.6×10^{-8} for NWC
C_1 = 5.0×10^{-6} for HWC, 5.0×10^{-5} for NWC
n = 3 for HWC, 2.5 for NWC

In this calculation, the IGSCC growth law for normal water chemistry (NWC) is conservatively used instead of law for hydrogen water chemistry (HWC).

4.3.2 *Stainless Steel IGSCC Growth Law*

BWRVIP-14-A [13, Equation 3-4] provides stress corrosion crack growth laws for austenitic steel in a BWR water chemistry conditions. In this evaluation, the IGSCC growth laws for hydrogen water chemistry shown in Equation (5) below are used if IGSCC is active.

$$\ln\left(\frac{da}{dt}\right) = 2.181 \cdot \ln(K_I) - 0.787 \cdot Cond^{-0.586} + 0.00362 \cdot ECP + \frac{6730}{T_{ABS}} - 33.235 \quad (5)$$

where,

da/dt = crack growth rate, mm/s (multiply by 141.73 for in/hr)
K_I = stress intensity factor at flaw tip, MPa√m
Cond = average conductivity, μS/cm
ECP = electrochemical corrosion potential, mV(SHE)
T_{ABS} = temperature, K

From BWRVIP-14-A [12, page 1-2] the average conductivity (Cond) and electrochemical corrosion potential (ECP) for hydrogen water chemistry is <0.15 μS/cm and ≤-230 mV(SHE), respectively.

The Equation (5) can be converted to the following equation in **pc-CRACK** (Paris formulation).

$$\frac{da}{dt} = C \cdot K_I^{\,n}$$

where,

C = 4.819×10^{-8}
n = 2.181

The calculations for C and n of above equation are given in Excel spreadsheet, *1500503.316.xlsm*.

4.4 Treatment of Negative Stress Intensity Factors for FCG

Because of the beneficial compressive residual stresses produced by the weld overlay, the stress intensity factors for many load cases are negative. This condition is handled as follows in the FCG analyses:

1. For Alloy 600 and its weld metals (Alloy 82/Alloy 182), the crack growth law in Equation (1) includes an R-ratio corrector factor $(1\text{-}0.82R)^{-2.2}$ that applies to both positive and negative R-ratios [10]. For negative R-ratios, the factor is less than 1, yielding a corresponding decrease in crack growth rate. Therefore, Equation (1) is used directly for crack growth in the DMW when K_{max} is greater than zero, for both positive and negative K_{min}.
2. If both K_{max} and K_{min} in a load cycle are negative, zero fatigue crack growth is assumed. This is a reasonable assumption based on the work on compression fatigue crack growth (FCG for which K_{max} and K_{min} are negative) in Reference 14, in which it was shown that although FCG is present, the values of FCG are several orders of magnitude smaller than for FCG for which K_{max} and K_{min} are not negative.

Due to the significant compressive stresses applied by the FSWOL, as seen in Figure 6, there is a high likelihood that the K_{max} and K_{min} values for the transients defined in Table 2 will both be negative. As stated above, if both K values are negative, there is no crack growth. However, **pc-CRACK** does not have the capability to turn off the crack growth laws defined in Section 4.2 for this condition. Therefore, as an initial test, the **pc-CRACK** evaluations are initially only run for 1 year of FCG and IGSCC.

The K_{max} and K_{min} values at 75% of the base metal thickness for all of the transients and the steady state conditions (used for IGSCC) were extracted for both the circumferential and axial flaws, and are shown in Table 3.

Table 4 shows the extracted K_{max} and K_{min} values at 100% of the original base metal thickness for just the axial flaw. The base metal thickness of 1.203 inches was again used, despite the fact that the surface indication was partially excavated and refilled to minimize any chance of cracking during the FSWOL application process. Because the initial flaw is 100% through the base metal thickness, the Alloy 52M crack growth law and IGSCC growth laws should be used to determine the crack growth into the overlay. However, since the Ks are all negative, the use of the Alloy 182 laws in the **pc-CRACK** evaluation does not alter the results.

In all cases, the K values are negative, indicating that there will be no crack growth due to FCG or IGSCC for either the 75% through-wall axial or circumferential flaw or the 100% through-wall axial flaw.

5.0 RESULTS OF ANALYSIS

The crack growth results for an initial flaw of 75% of the original base metal thickness are shown in Table 5 and Table 6. At the DMW, it takes greater than 40 years for an initial flaw of 75% of the original base metal thickness at the analyzed section to reach the overlay for both the circumferential flaw and axial flaw. Similarly, in the heat affected zone of the stainless steel safe end, it takes greater than 40 years for an initial flaw of 75% of the original base metal thickness at the analyzed section to reach the overlay for both the circumferential flaw and axial flaw.

For an initial axial flaw of 100% of the original base metal thickness, it takes greater than 40 years to reach 75% of the total thickness (base metal plus FSWOL) as shown in Table 7.

IGSCC is not active in the original base metal for both the 75% through-wall circumferential and axial flaws and the 100% through-wall axial flaw, since Ks at steady state NOC are negative for all flaw depths. Figure 6 shows an example of Ks at steady NOC for Path 3.

6.0 REFERENCES

1. SI Calculation No. 1500503.313, "Thermal and Mechanical Stress Analyses of the Recirculation Inlet Nozzle Weld Overlay Repair," (for revision number refer to SI Project Revision Log, latest revision).
2. SI Calculation No. 1500503.314, "Weld Residual Stress Analysis of the Recirculation Inlet Nozzle Weld Overlay," (for revision number refer to SI Project Revision Log, latest revision).
3. ASME Boiler and Pressure Vessel Code, Code Case N-740-2, "Full Structural Dissimilar Metal Weld Overlay for Repair on Mitigation of Class 1, 2, and 3 Items, Section XI, Division 1."
4. Southern Nuclear Operating Company Proposed Alternative HNP-ISI-ALT-15-01, "Edwin I. Hatch Nuclear Plant – Unit 1, Proposed Alternative in Accordance with 10CFR 50.55a(z)(1), Application of Dissimilar Weld Full-Structural Weld Overlays," dated July 2, 2015, SI File No. 1500503.205.
5. SI Calculation No. 1500503.311, "Loop B Recirculation Inlet Nozzles N2C and N2E Design Loads," (for revision number refer to SI Project Revision Log, latest revision).
6. SI Calculation No. 1500503.312, "Finite Element Model Development of the Recirculation Inlet Nozzle Weld Overlay," (for revision number refer to SI Project Revision Log, latest revision).
7. **pc-CRACK** 4.1 CS, Version Control No. 4.1.0.0, Structural Integrity Associates, December 31, 2013.
8. **SI-TIFFANY** 3.0, Structural Integrity Associates, September 15, 2015.
9. ASME Boiler and Pressure Vessel Code, Section XI, Rules for Inservice Inspection of Nuclear Power Plant Components, 2001 Edition through 2003 Addenda.
10. NUREG/CR-6721, "Effects of Alloy Chemistry, Cold Work, and Water Chemistry on Corrosion Fatigue and Stress Corrosion Cracking of Nickel Alloys and Welds," U.S. Nuclear Regulatory Commission (Argonne National Laboratory), April 2001.
11. Section XI Task Group for Piping Flaw Evaluation, ASME Code, "Evaluation of Flaws in Austenitic Steel Piping," Journal of Pressure Vessel Technology, Vol. 108, August 1986.
12. *BWRVIP-59-A: BWR Vessel and Internals Project, Evaluation of Crack Growth in BWR Nickel Base Austenitic Alloys in RPV Internals*. EPRI, Palo Alto, CA, May 2007, 1014874.
13. *BWRVIP-14-A: BWR Vessel and Internals Project, Evaluation of Crack Growth in BWR Stainless Steel RPV Internals*. EPRI, Palo Alto, CA: 2008. 1016569.
14. Lenets, Y. N., "Compression Fatigue Crack Growth Behavior of Metallic Alloys: Effect of Environment," Engineering Fracture Mechanics, Vol. 52, No. 5, 1997.
15. GE HITACHI UT Examination Summary Sheet, Report No. H1R27-APR-07, Weld No. 1B31-1RC-12BR-E-5, SI File No. 1500503.213
16. AZZ/WSI Drawing No. 429860, Rev. 2, "Drawing, Construction, Nozzle, Recirc Inlet, Hatch," SI File No. 1500503.212.

17. SI Drawing No. 1500503.510, "Hatch 1 Recirculation Inlet Nozzle Weld Overlay," (for revision number refer to SI Project Revision Log, latest version).

Table 1: Recirculation Inlet Nozzle Bounding Piping Loads

Load Type	Force (lb)			Moment (in-lb)		
	FA	FB	FC	MA	MB	MC
THERMAL[1]	-595	-5037	-9841	387204	470887	191888
WEIGHT	995	6431	120	10196	12866	-250613
SEISMIC[2]	1143	442	911	39284	61710	56919
OBED[2]	158	-57	1722	-72713	73450	6210

Notes:

1. The piping expansion loads for a desired temperatures will use a scale factor based on a temperature of 535°F.
2. The term SEISMIC is for the inertial component of OBE, while OBED is the seismic anchor movement component of OBE.

Table 2: Bounding Thermal Transients for the Recirculation Inlet Nozzle

Abbreviation	ID	Cycle Description	No of Cycles[2]	Annual Cycles	Internal Cycles	Pressure (psig)		Temp (°F)	
						Max.	Min.	Max.	Min.
7SS	"2-3"	Hydro Test	130	3.25	1	1424	0	101	101
1HUTR	"3-4"+ Part of "4-5"	Start up + First Part of Turbine Roll & Increase to Power	120	3	2	1223	0	553	101
2TR	Second Part of "4-5"	Second Part of Turbine Roll and Increase to Power	120	3	1	1223	1223	545	535
3TT	"9-10"	Turbine Trip at 25% Power	20	0.5	1	1223	1223	545	535
4FWHB	"10-11"	Feedwater Heater Bypass	70	1.75	1	1223	1223	535	519
8LOSS	"11-12"	Loss of FW Pumps ISOL Valves Close	10	0.25	5	1353	411	553	304
5SCRAM	"12-13" & "15-16"	SCRAM (Upset)	187	4.675	3	1298	411	553	405
6SDN	"21-24"	Shutdown Normal	120	3	2	1223	205	535	101
	"37-38"	Operating Basis Earthquake (OBE) [3]	600			1223	1223	N/A	N/A

Notes:

1. The information shown in the table above is from Table 5 of Reference 5.
2. Cycles based on 40 year design life.
3. OBE is added to the K_{max} for the maximum value and subtracted from K_{min} for the minimum value of each transient.

Table 3: Stress Intensity Factors at 75% of Original Base Metal Thickness

Abbreviation	ID	Cycle Description	Circumferential Flaw											
			P3 (1)		P4		P5		P8 (1)		P9		P10	
			K_{max}	K_{min}	K_{max}	K_{min}	K_{max}	K_{min}	K_{max}	K_{min}	K_{max}	K_{min}	K_{max}	K_{min}
1HUTR	"3-4"+ Part of "4-5"	Start up + First Part of Turbine Roll & Increase to Power	-12.65	-34.48	-24.10	-41.23	-30.50	-44.73	-9.49	-34.55	-20.62	-41.30	-26.71	-44.78
2TR	Second Part of "4-5"	Second Part of Turbine Roll and Increase to Power	-19.84	-23.35	-26.89	-30.35	-30.60	-34.10	-16.87	-20.37	-23.62	-27.08	-27.04	-30.53
3TT	"9-10"	Turbine Trip at 25% Power	-19.87	-23.38	-26.95	-30.44	-30.67	-34.19	-16.90	-20.39	-23.68	-27.15	-27.11	-30.62
4FWHB	"10-11"	Feedwater Heater Bypass	-19.76	-23.45	-26.90	-30.73	-30.72	-34.74	-16.78	-20.45	-28.18	-27.42	-27.15	-31.14
5SCRAM	"12-13" & "15-16"	SCRAM (Upset)	-16.79	-29.12	-25.10	-36.03	-29.58	-39.78	-13.63	-28.17	-21.63	-34.97	-25.80	-38.61
6SDN	"21-24"	Shutdown Normal	-12.32	-33.02	-23.06	-39.70	-27.96	-43.39	-9.27	-32.69	-19.75	-39.31	-24.38	-42.80
7SS	"2-3"	Hydro Test	-16.64	-34.33	-28.17	-40.76	-34.58	-44.28	-13.01	-34.56	-24.15	-40.97	-30.42	-44.32
8LOSS	"11-12"	Loss of FW Pumps ISOL Valves Close	-13.87	-30.30	-21.93	-37.17	-25.09	-40.92	-10.61	-29.36	-18.34	-36.08	-21.19	-39.74
IGSCC			-16.18		-21.91		-27.19		-16.23		-21.92		-27.21	

Abbreviation	ID	Cycle Description	Axial Flaw											
			P3 (1)		P4		P5		P8 (1)		P9		P10	
			K_{max}	K_{min}	K_{max}	K_{min}	K_{max}	K_{min}	K_{max}	K_{min}	K_{max}	K_{min}	K_{max}	K_{min}
1HUTR	"3-4"+ Part of "4-5"	Start up + First Part of Turbine Roll & Increase to Power	-94.49	-128.1	-97.53	-126.2	-98.54	-124.7	-95.69	-128.1	-98.41	-126.1	-99.06	-124.7
2TR	Second Part of "4-5"	Second Part of Turbine Roll and Increase to Power	-94.75	-94.92	-97.55	-97.75	-98.54	-98.83	-95.91	-96.11	-98.40	-98.64	-99.03	-99.36
3TT	"9-10"	Turbine Trip at 25% Power	-94.86	-94.96	-97.65	-97.83	-98.62	-98.96	-96.01	-96.16	-98.50	-98.73	-99.11	-99.50
4FWHB	"10-11"	Feedwater Heater Bypass	-95.07	-95.74	-97.71	-98.50	-98.57	-99.55	-96.23	-96.97	-98.57	-99.44	-99.06	-100.1
5SCRAM	"12-13" & "15-16"	SCRAM (Upset)	-93.90	-108.5	-96.81	-109.9	-97.88	-110.2	-95.12	-108.7	-97.71	-112.2	-98.41	-110.3
6SDN	"21-24"	Shutdown Normal	-95.38	-126.4	-98.10	-124.3	-99.07	-122.9	-96.55	-126.6	-98.98	-124.4	-99.58	-123.0
7SS	"2-3"	Hydro Test	-92.35	-128.5	-95.35	-126.1	-96.73	-124.8	-93.72	-128.4	-96.38	-126.1	-97.34	-124.8
8LOSS	"11-12"	Loss of FW Pumps ISOL Valves Close	-90.60	-113.0	-91.69	-113.0	-91.56	-113.0	-91.57	-113.1	-92.35	-113.1	-91.82	-112.9
IGSCC			-86.09		-89.21		-90.74		-86.05		-89.21		-90.74	

Note: (1) Stress intensity factors for Paths P3 and P8 represent both the Alloy 182 and stainless steel regions.

Table 4: Stress Intensity Factors at 100% of Original Base Metal Thickness for Axial Flaw

Abbreviation	ID	Cycle Description	Axial Flaw											
			P3		P4		P5		P8		P9		P10	
			K_{max}	K_{min}	K_{max}	K_{min}	K_{max}	K_{min}	K_{max}	K_{min}	K_{max}	K_{min}	K_{max}	K_{min}
1HUTR	"3-4"+ Part of "4-5"	Start up + First Part of Turbine Roll & Increase to Power	-89.18	-131.6	-70.55	-105.9	-86.48	-116.1	-90.61	-131.6	-71.63	-105.9	-87.22	-116.1
2TR	Second Part of "4-5"	Second Part of Turbine Roll and Increase to Power	-89.03	-88.98	-70.39	-70.40	-86.33	-86.45	-90.48	-90.47	-71.47	-71.51	-87.05	-87.20
3TT	"9-10"	Turbine Trip at 25% Power	-89.11	-88.99	-70.49	-70.44	-86.40	-86.55	-90.57	-90.48	-71.56	-71.55	-87.12	-87.32
4FWHB	"10-11"	Feedwater Heater Bypass	-89.50	-89.76	-70.64	-71.05	-86.32	-87.00	-90.97	-91.28	-71.73	-72.21	-87.05	-87.80
5SCRAM	"12-13" & "15-16"	SCRAM (Upset)	-87.86	-106.5	-69.38	-85.86	-85.46	-100.4	-89.41	-106.8	-70.53	-91.10	-86.24	-100.4
6SDN	"21-24"	Shutdown Normal	-89.57	-128.8	-70.84	-103.2	-86.71	-113.6	-91.06	-129.1	-71.91	-103.4	-87.46	-113.7
7SS	"2-3"	Hydro Test	-85.14	-131.1	-67.08	-105.5	-83.68	-115.9	-86.91	-131.1	-68.35	-105.5	-84.57	-115.9
8LOSS	"11-12"	Loss of FW Pumps ISOL Valves Close	-86.21	-111.7	-65.98	-89.44	-79.94	-103.2	-87.80	-111.9	-66.94	-89.59	-80.51	-103.2
IGSCC			-75.22		-59.61		-73.33		-75.40		-59.66		-73.37	

Table 5: Crack Growth Results – Alloy 182

Flaw Type	Path	Time for Initial Flaw Depth to Reach Overlay
Circumferential Flaw	P3	> 40 years
	P4	
	P5	
	P8	
	P9	
	P10	
Axial Flaw	P3	> 40 years
	P4	
	P5	
	P8	
	P9	
	P10	

Note:
1. Initial flaw depth = 75% of original base metal thickness at the section analyzed
= 0.9024 inches

Table 6: Crack Growth Results – Stainless Steel

Flaw Type	Path	Time for Initial Flaw Depth to Reach Overlay
Circumferential Flaw	P3	> 40 years
	P8	
Axial Flaw	P3	
	P8	

Note:
1. Initial flaw depth = 75% of original base metal thickness at the section analyzed
= 0.9024 inches

Table 7: Crack Growth Results for Initial Flaw of 100% of Original Base Metal Thickness

Flaw Type	Path	Time for Initial Flaw Depth to Reach 75% of Total Thickness (Base Metal + FSWOL)
Axial Flaw	P3	> 40 years
	P4	
	P5	
	P8	
	P9	
	P10	

Note:

1. Initial flaw depth = 100% of original base metal thickness at the section analyzed
   = 1.203 inches
2. The Alloy 182 fatigue crack growth laws and IGSCC growth were entered instead of the Alloy 52M laws. However, since the stress intensity factors are all negative, no crack growth from either source is possible.

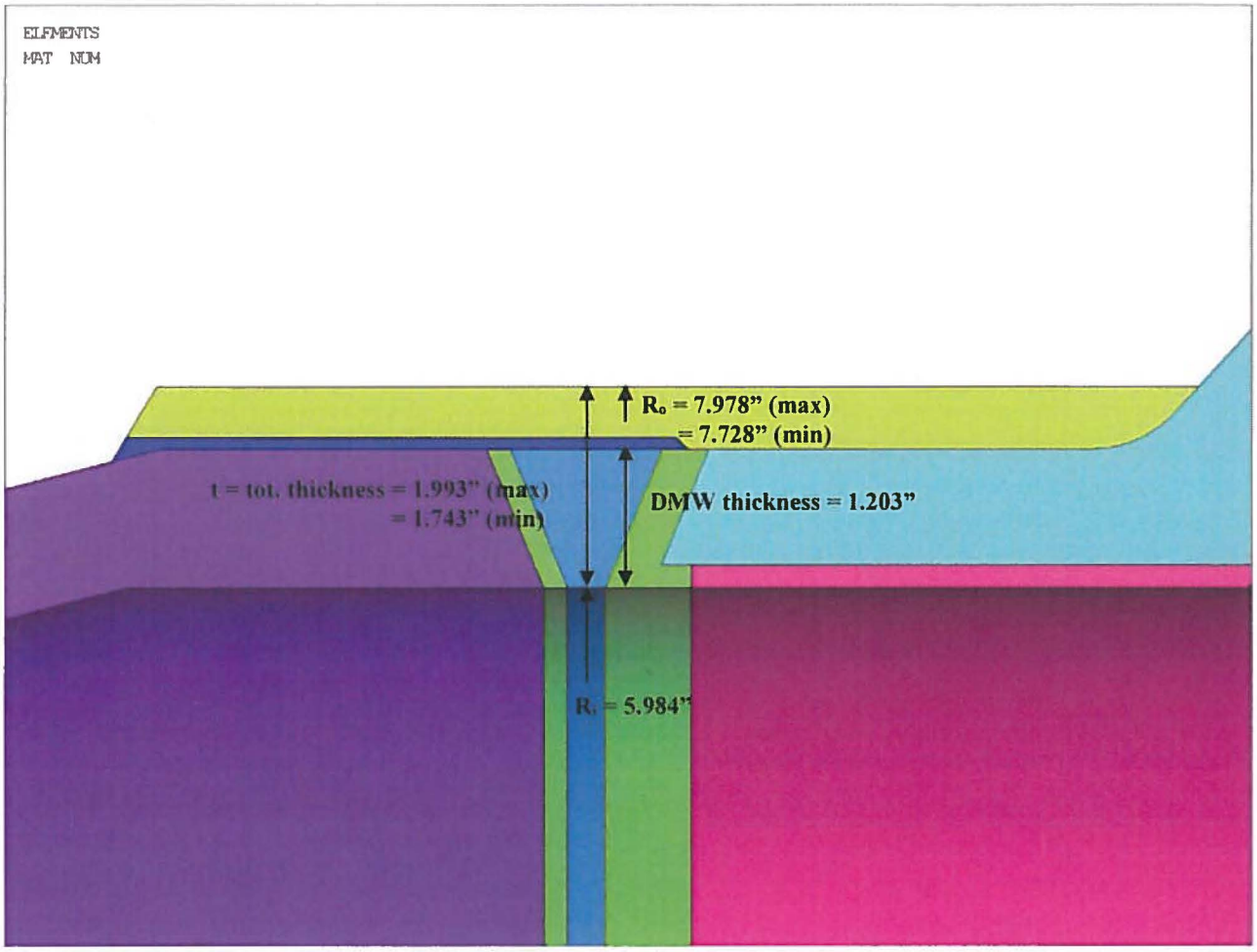

Figure 1. Section Dimensions Used For Crack Growth Calculations

Note: Dimensions were obtained from the finite element models developed in Reference 6.

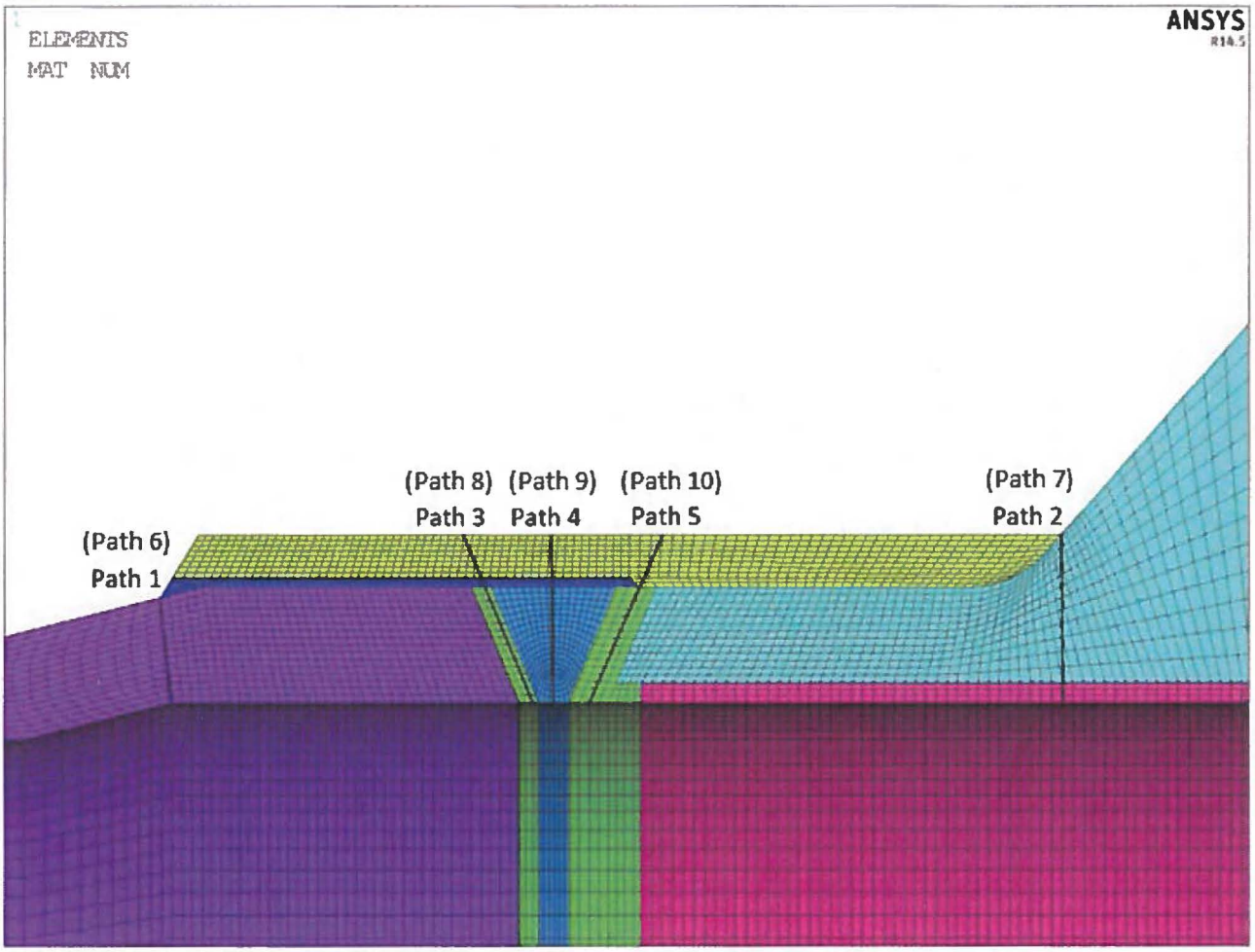

Figure 2. Paths within the DMW for Through-Wall Stress Extraction

Note: Paths 3 through 5 are along the paths shown. Paths 8 through 10 indicate corresponding paths located 90° from the above locations.

Figure is from reproduced from Reference 1.

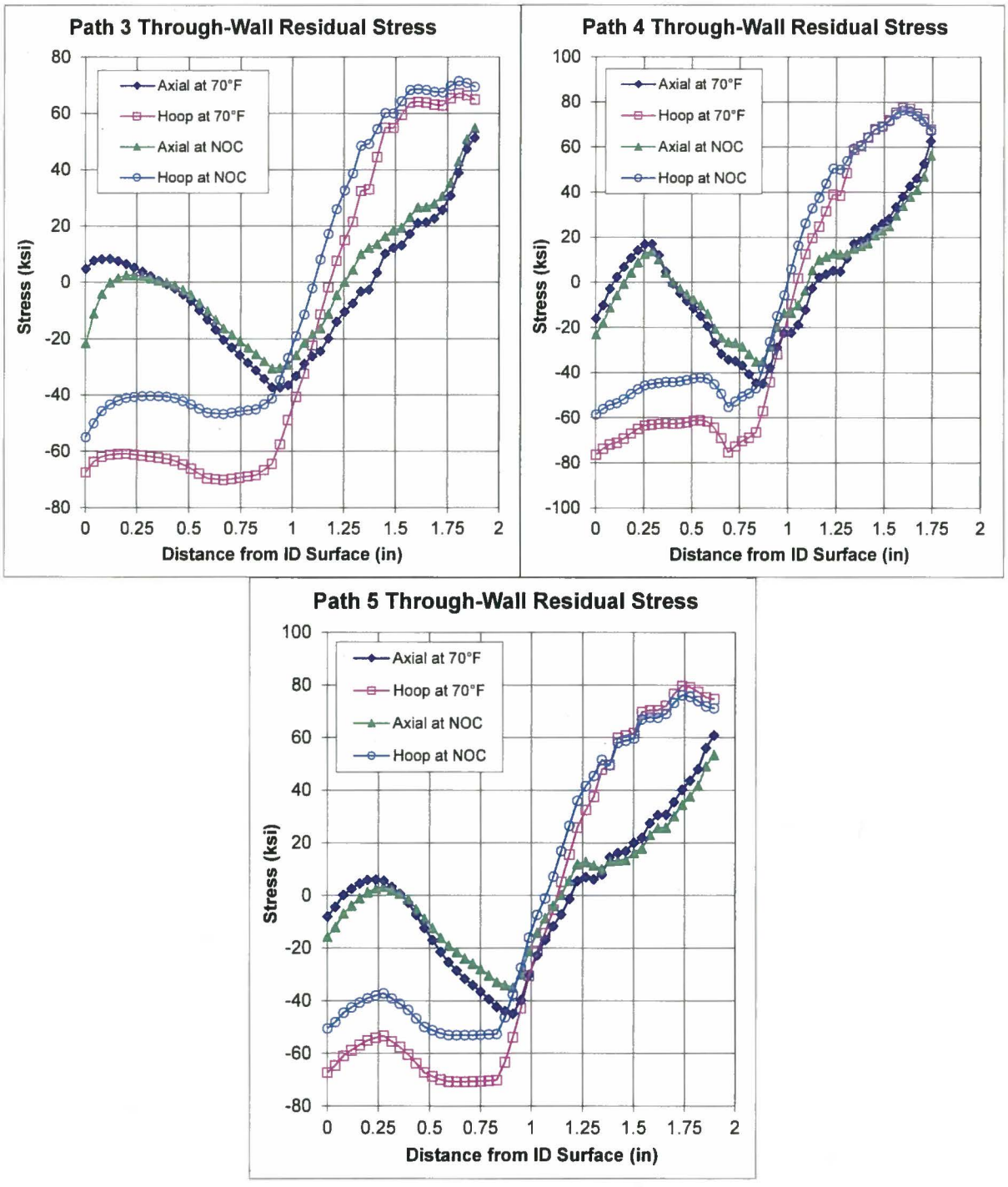

Figure 3. Through-Wall Weld Residual Stress Distributions at 70°F and NOC for the DMW

Crack Model: 301 - Full-Circumferential Crack in Cylinder on the Inside Surface

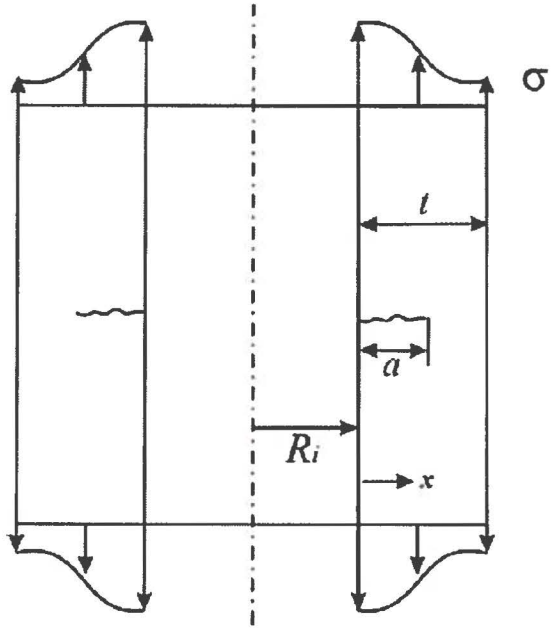

Stress/Load Input	
Stress Coefficients	✓
Coeffs. from Stress Table	✓
Stress Table	✓
Stress Intensity Factors (1D)	✓
Stress Intensity Factors (2D)	×
Crack Dimensions: a Component Dimensions: t R_i	
Range: $0.0 < a/t \leq 0.8$ $0 < R_i/t \leq 1000$ Source: [11]	

Figure 4. pc-CRACK Full-Circumferential Crack Model for Stress Intensity Distribution Calculation due to Axial Stress

(Figure from pc-CRACK 4.1 CS User's Manual [7])

Crack Model: 305 - Semi-Elliptical Longitudinal Crack in Cylinder on the Inside Surface (API 579)

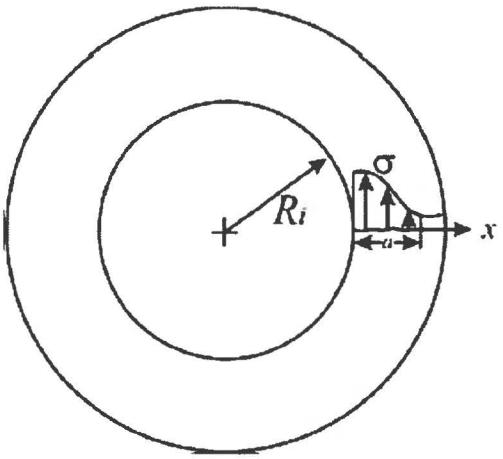

Stress/Load Input		
Stress Coefficients		✓
Coeffs. from Stress Table		✓
Stress Table		✓
Stress Intensity Factors (1D)		✓
Stress Intensity Factors (2D)		✓
Crack Dimensions:	a	c
Component Dimensions:	t	R_i
Range:		
$0.0 < a/t \leq 0.8$		
$0.03125 \leq a/c \leq 2.0$		
$0.0 < t/R_i \leq 1.0$		
Source: [11]		

Figure 5. pc-CRACK Semi-Elliptical Longitudinal Crack in Cylinder on the Inside Surface for Stress Intensity Distribution Calculation due to Hoop Stress

(Figure from pc-CRACK 4.1 CS User's Manual [7])

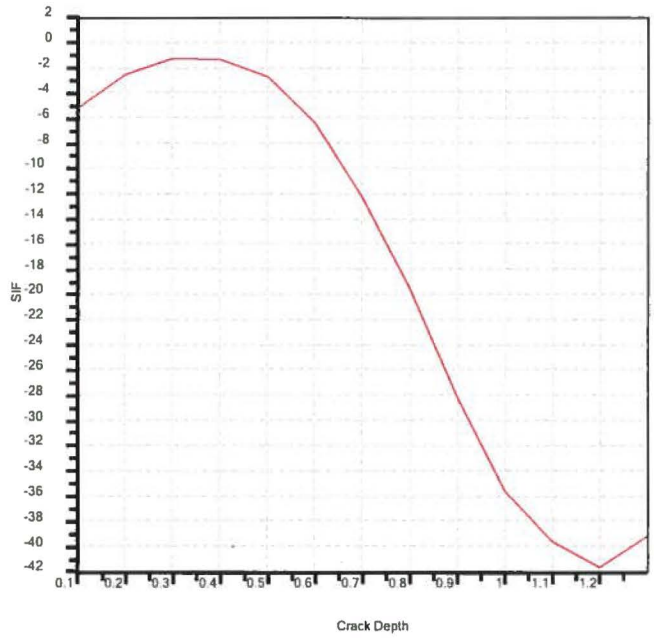

Circumferential Flaw

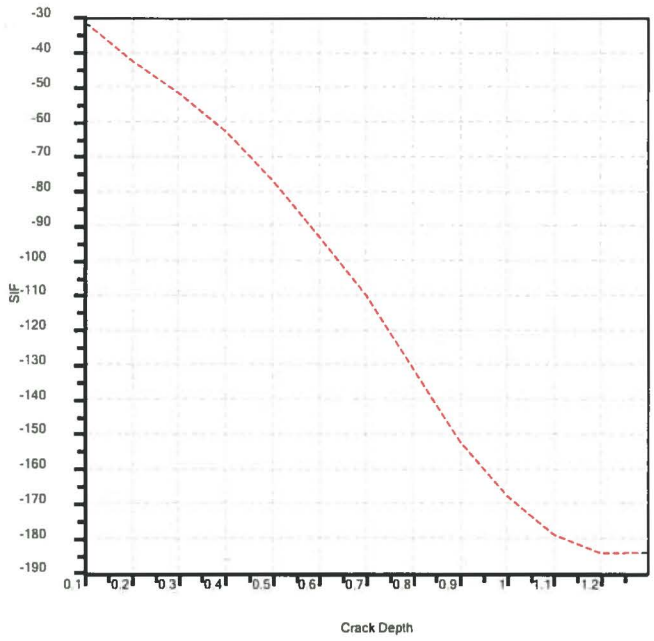

Axial Flaw

Figure 6. K Distributions at Steady State NOC at Path 3

APPENDIX A

COMPUTER FILES

SI-TIFFANY Files

File Name	Description
P*_$$$_##.dat	**SI-TIFFANY** input file to determine maximum and minimum K values (* = 3, 4, 5, 8, 9, and 10 for path number, $$$ = 1HUTR, 2TR, 3TT, 4FWHB, 5SCRAM, 6SDN, 7SS, and 8LOSS for transient whose abbreviations are in Table 2, and ## = axial and circumferential for flaw type)
P*_$$$_##.rpt	**SI-TIFFANY** main output file (see above description for *, $$$, and ##)
P*_$$$_##.mxn	**SI-TIFFANY** output file with maximum K values (see above description for *, $$$, and ##)
P*_$$$_##.mnn	**SI-TIFFANY** output file with minimum K values (see above description for *, $$$, and ##)
P*_$$$_##.kvt	**SI-TIFFANY** output file with K values as a function of time (see above description for *, $$$, and ##)
STR_$$$_MAP_P*.csv	Mapped component stress outputs in tabulated forms from Reference 1. Stress outputs are read by SI-TIFFANY. (see above description for * and $$$)

pc-CRACK Files

File Name	Description
P*-##.pcf	**pc-CRACK** input file to evaluate crack growth (* = 3, 4, 5, 8, 9, and 10 for path number and ## = axial and circumferential for flaw type)
P*-##.rpt	**pc-CRACK** main output file (see above description for * and ##)
P*-##.avc	**pc-CRACK** output file (see above description for * and ##)
P*-##.avn	**pc-CRACK** output file (see above description for * and ##)
P*-##.kva	**pc-CRACK** output file (see above description for * and ##)
P*_$$$_##.mxn	**SI-TIFFANY** output file with maximum K values (see description in SI-TIFFANY Files Table)
P*_$$$_##.mnn	**SI-TIFFANY** output file with minimum K values (see description in SI-TIFFANY Files Table)
STR_PRESS_MAP_P*.csv	Mapped component stress outputs due to unit pressure in tabulated forms form Reference 1 (* = 3, 4, 5, 8, 9, and 10 for path number)
STR_FORCEY_MAP_P*.csv	Mapped component stress outputs due to unit axial force in tabulated forms from Reference 1 (* = 3, 4, 5, 8, 9, and 10 for path number)
STR_MOMENT%_MAP_P*.csv	Mapped component stress outputs due to unit lateral moment in tabulated forms from Reference 1 (* = 3, 4, 5, 8, 9, and 10 for path number and % = X and Z for direction of the moment)
STRESS2D_MAP_P*.csv	Mapped component residual stress output from Reference 2 (* = 3, 4, and 5 for path number)
P*-Axial_100.pcf	**pc-CRACK** input file to evaluate crack growth for 100% through-wall initial axial flaw (* = 3, 4, 5, 8, 9, and 10 for path number)
P*-Axial_100.rpt	**pc-CRACK** main output file for 100% through-wall initial axial flaw (see above description for *)
P*-Axial_100.avc	**pc-CRACK** output file for 100% through-wall initial axial flaw (see above description for *)
P*-Axial_100.avn	**pc-CRACK** output file for 100% through-wall initial axial flaw (see above description for *)
P*-Axial_100.kva	**pc-CRACK** output file for 100% through-wall initial axial flaw (see above description for *)

Supporting Files

File Name	Description
1500503.316.xlsm	Excel spreadsheet for generating SI-TIFFANY input files, calculating material properties for crack growth laws, and determining scale factors for unit pressure, force, and moment